Imaging of the Porous Ultrastructure of the Glomerular Epithelial Filtration Slit

Elena Gagliardini,* Sara Conti,* Ariela Benigni,* Giuseppe Remuzzi,*[†] and Andrea Remuzzi*[‡]

*Mario Negri Institute for Pharmacological Research, Centro Anna Maria Astori, Science & Technology Park Km Rosso, Bergamo, Italy; [†]Unit of Nephrology, Azienda Ospedaliera, Ospedali Riuniti di Bergamo, Bergamo, Italy; and [‡]Industrial Engineering Department, University of Bergamo, Dalmine, Italy

ABSTRACT

The ultrastructure of the glomerular filtration slit is still controversial. In the last 30 years, observations from transmission electron microscopy (TEM) and theoretical analysis of solute clearance produced conflicting results. Here, we used scanning EM with a high-sensitivity detector to image the deepest regions of the filtration slits and report a previously undescribed organization of the slits' ultrastructure. In contrast to previous TEM imaging, we observed circular and ellipsoidal pores in the podocyte junctions mainly located in the central region of the slit diaphragm. The normal mean pore radius estimated by digital morphometric analysis had a log-normal distribution, with an average value of 12.1 nm. In proteinuric pathologic conditions, the mean pore radius values were also log-normally distributed with the presence of some very large pores, exceeding the sizes observed in normal conditions. Our morphologic analysis suggests that the filtration slit is a heteroporous structure instead of the previously proposed zipper-like structure. Selective changes in the ultrastructural organization of the pores may be responsible for the increased filtration of plasma proteins in glomerular disease.

The permeability properties of the glomerular capillary wall allow the filtration of high water flow and small solutes but efficient retention of plasma proteins the size of albumin or larger.[1] It has been indicated that most of the restriction of macromolecule ultrafiltration is caused by the epithelial filtration slits, because plasma proteins can cross endothelial cells and glomerular basement membrane (GBM) more easily.[2] Changes in glomerular permselective function resulting in increased glomerular filtration of plasma proteins and incomplete tubular reabsorption are responsible for loss of proteins in the urine. These events have been linked to the progression of renal diseases.[3] With the aim to characterize the mechanisms behind proteinuria, in the last 30 years, solute clearance techniques have been used to estimate the selective properties of the glomerular barrier in experimental models of nephropathy and in patients. In particular, glomerular size-selective function has been studied using renal clearance of neutral test macromolecules (*i.e.*, neutral dextran and Ficoll) that are not secreted or reabsorbed at the tubular level. Theoretical models of glomerular size selectivity have been conventionally used to derive intrinsic membrane selective properties from fractional clearance of test macromolecules in terms of density and size of hypothetical pores perforating the glomerular capillary wall.[2,4,5] Thus, according to the two-pore

theory, in the normal rat, the radius of small pores is in the range of 4.5 to 5.0 nm and that of large pores is between 8.0 and 10.0 nm.[6] Similarly, according to the lognormal pore radii distribution model, the mean pore radius is in the range of 3.5 and 4.5 nm, and the largest pores of the distribution have radii up to 8.0 nm or larger.[5] According to these pore dimensions, albumin, which has a molecular radius of 3.6 nm, should be filtered across the glomerular capillary wall almost exclusively through the largest pores that are few in number. This is in line with the observation that fractional clearance (*i.e.*, ultrafiltrate to plasma concentration ratio) of albumin in the rat in normal conditions is <0.004.[7–10] The estimation of the dimension of hypothetical pores of the glomerular capillary membrane has been successfully used to investigate disease processes and effects of pharmacologic treatments on glomerular permselectivity. However, these evaluations are not consistent with the dimensions of pores derived from electron microscopy (EM) studies of the outer layer of the glomerular membrane, the epithelial filtration slits. The first detailed documentation of the ultrastructural organization of glomerular epithelial cell junction was provided by Rodewald and Karnowsky in the 1970s[11] using transmission EM (TEM). These authors suggested a geometric model of the organization of the filtration slit based on a "zipper-like" structure, in which the slit diaphragm is composed by regularly spaced rod-like units extending from the lateral membrane of two adjacent podocyte foot processes to a linear central bar, running longitudinally and parallel to the cell membranes. The distance between the adjacent foot processes membrane was calculated to be 39 nm, in line with more recent reports,[12–15] and the central filament width was calculated to be 11 nm in diameter. The slit diaphragm was suggested to contain rectangular apertures of 4 × 14 nm, originating from filaments perpendicular to the cell membrane. For a long time, this zipper-like model represented a basic concept in capillary wall ultrastructure morphology. However, the dimensions of the apertures originally proposed through which water and circulating macromolecules would cross the glomerular membrane are not compatible with the documented filtration of albumin and test macromolecules in normal conditions.[7] From crystallographic analysis, the dimensions of albumin are 5.97 × 9.70 × 5.97 nm, as reported in Protein Data Bank.[16] The mean hydrodynamic diameter of albumin was reported to be 7.2 nm.[17] Micropuncture data suggest that some albumin does escape the glomerular membrane even in normal conditions, with a concentration, in the early proximal tubule fluid, ranging from 20 to 30 mg/ml.[18] The dimension of the apertures of the slit structure proposed by Rodewald and Karnovsky (only 4 nm wide) would not be consistent with albumin passage across an intact slit structure; in this case, only protein recycling by glomerular cells could explain the presence of albumin in ultrafiltrate fluid.

More recently, Hora *et al.*[19] examined normal rat glomeruli by the quick-freezing and deep-etching replica method and suggested that the glomerular slit diaphragm has a sheet-like structure rather than a zipper-like structure. These authors, however, did not derive measurements of openings present in the slit diaphragm. Tryggvason *et al.*[15] provided new insight into the three-dimensional molecular structure of the podocyte slit diaphragm by the identification of the proteins that compose the glomerular epithelial junction and the use of EM tomography. They suggested a 40-nm-wide slit diaphragm structure with a network of convoluted strands forming the scaffold of the slit diaphragm. In this model, the strands are positioned at different levels of the slit and are in contact each other in their central region, forming irregular pores.[15] The strands observed in these experiments are wavy and irregularly spaced, at variance with the model of Rodewald and Karnovsky. Nevertheless, the dimension of the openings available for filtration estimated in this study[15] is comparable to the original zipper-like model.[11]

In this study, we took advantage of scanning EM (SEM) to directly investigate the outer side of the glomerular filtration slit. Morphologic analysis of the filtration slits by SEM has been limited thus far by difficulties in capturing secondary electrons (those scattered by the sample surface) that, for the three-dimensional geometry of the foot processes junction, are only minimally scattered toward the detector; the resulting images of the inner part of the slit always result in a dark area.[20] To overcome such limitations, we used a recently available SEM technique based on a more sensitive detector, the in-lens detector. Secondary electrons are more efficiently detected by this type of detector for the position nearer the scanned surface and the effect of acceleration obtained by the electromagnetic field of the lens.[21] These factors result in better signal-to-noise ratio. We took advantage of this innovative technology to study the deepest region of the filtration slits in an attempt to disclose its surface organization. We studied the filtration slits in normal physiologic conditions in the rat and in proteinuric conditions for comparison.

RESULTS

The In-Lens Detector Strengthens SEM Imaging

The analysis of cortical kidney samples of normal Wistar rats by SEM allowed us to image the outer surface of glomerular capillary and, in particular, the filtration slits with different results according to the detector used. As shown in Figure 1, photomicrographs taken with a conventional detector for secondary electrons (Figure 1, A–C) differ from those taken using an in-lens detector (Figure 1, D and E). Whereas at low magnification, a conventional detector allows one to obtain high-quality images, when at higher magnification, the filtration slits appear as a dark area (Figure 1C). On the contrary, the in-lens detector allowed visualization of the structure between two adjacent podocytes (Figure 1, D and E). In this area, we detected a network of strands forming irregular pores with a circular or ellipsoidal shape. These pores are mainly located in the central region of the filtration slit, and they appear heterogeneous in size and shape and are not regularly spaced. To rule
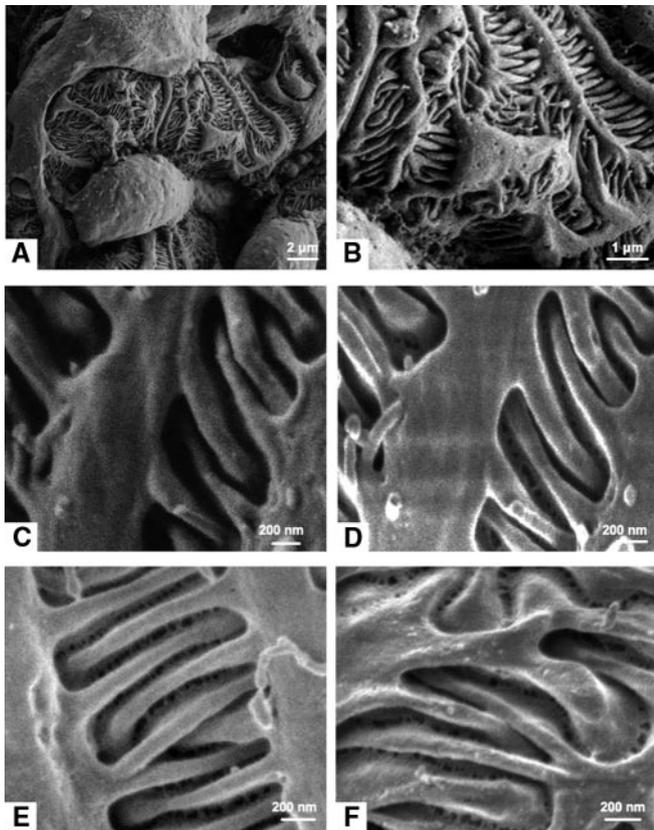
Figure 1. Visualization of epithelial filtration pores using an in-lens detector with SEM. Representative scanning electron photomicrographs from Wistar rat, taken at low and high magnifications (A: 12,000×; B: 36,000×; C and D: 60,000×; E: 80,000×; F: 100,000×) with conventional detector (A–C) and in-lens detector (D–F) for secondary electrons. In-lens photomicrographs of samples dehydrated with a critical point dryer (A–E) or HMDS (F).

out that the structures were an artifact caused by the dehydration process, we analyzed kidney samples dehydrated with hexamethyldisilazane (HMDS) to reach critical point dehydration less aggressively.[22,23] Renal specimens treated with HMDS (Figure 1F) showed the same heteroporous structure as samples dehydrated by a critical point dryer (Figure 1, D and E). In addition, to exclude the possibility that gold-coating could induce artifacts in the ultrastructure of the filtration slit, we also imaged uncoated samples of the peripheral glomerular capillary wall. As reported in Supplementary Figure S1, the same porous structure of the slit diaphragm was observed on both gold-coated and uncoated samples.

Morphometric Analysis in Healthy Rats

We estimated the dimension of pores detected in the podocyte slit regions of Wistar rats analyzing around 600 pores using digital morphometric analysis (Figure 2). Ellipsoidal pores have mean a minor and major radius of 9.8 and 14.7 nm, respectively. As shown in Figure 3A, the probability distribution of the mean pore radii is remarkably similar to the log-normal distribution. By best fit analysis of measured
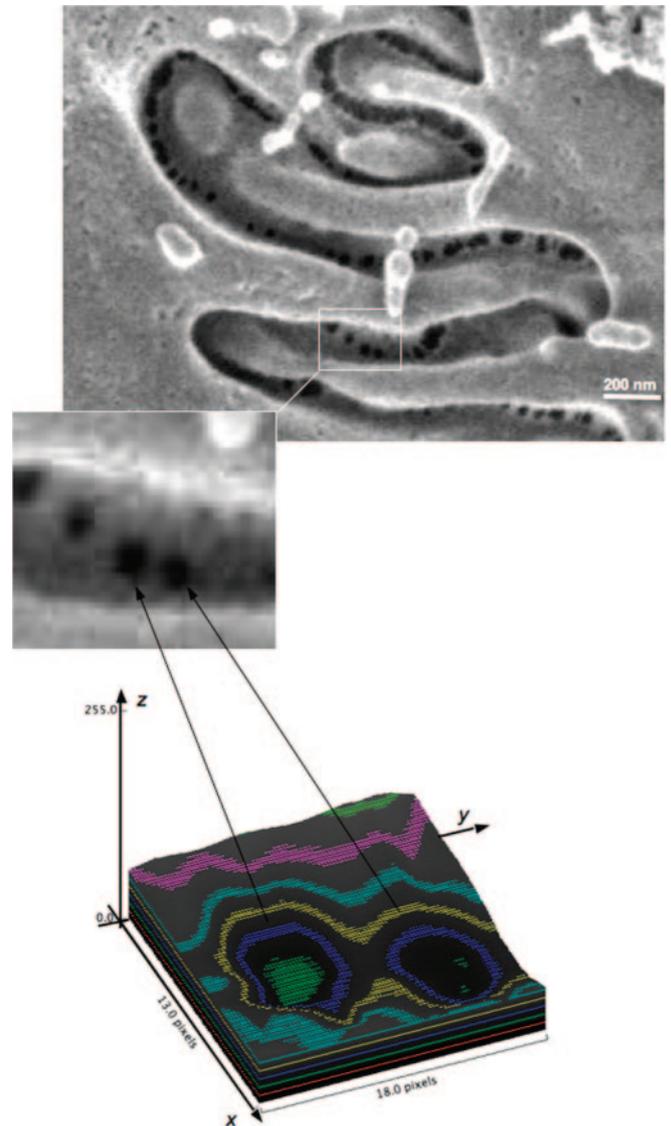

Figure 2. Schematic representation of the procedure used to evaluate pore dimension. (Top) A representative image obtained at scanning electron microscopy (original magnification, 200,000×) with an enlargement of the filtration slit pores. (Bottom) Representation of the surface plot obtained using the software Image J (v. 1.43 NIH).

values with log-normal probability distribution, we derived mean pore radius as $u = 12.1$ nm and an SD of the corresponding normal distribution as $s = 1.39$. To estimate the relative importance of pore size on water filtration, we calculated the distribution of fractional pore area (Figure 4A). Mean pore area was 494 nm^2, with a higher frequency of pore area ranging from 250 to 500 nm^2. The largest pores detected in normal rats has an area <2500 nm^2.

Renal Histology in MWF Rats

To study whether the organization of the filtration slits in proteinuric conditions is different from that in normal conditions, we studied kidney samples from Munich Wistar Frömter (MWF) rats. As shown in Table 1, consistently with
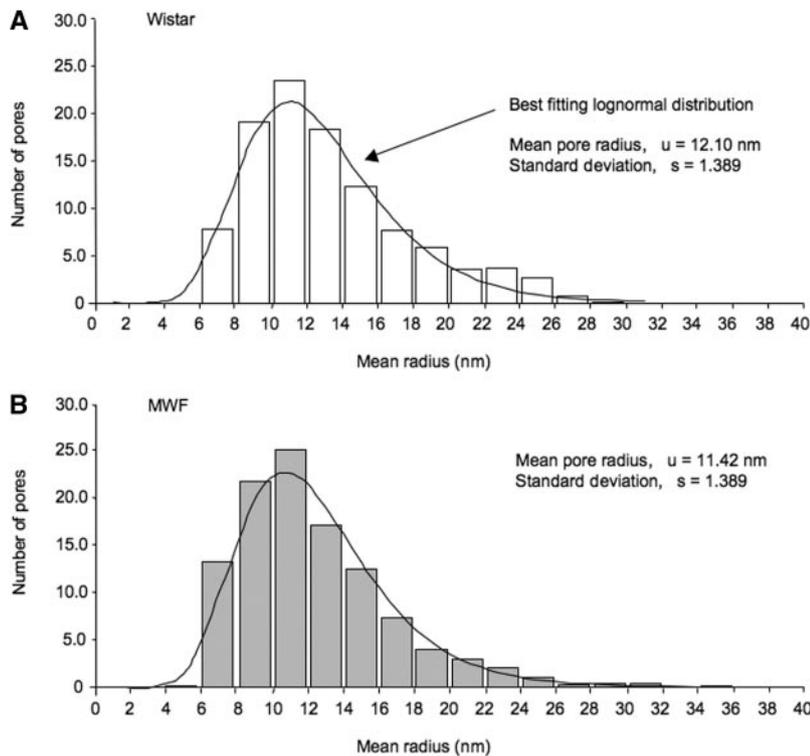
Figure 3. Distribution of slit pore size is unchanged under proteinuria. Distribution of slit pore sizes of Wistar (A) and MWF (B) rats, as measured by digital morphometric analysis and the best fit lognormal probability distribution of pore radii.

previous data,[24] 40-week-old MWF rats showed a significantly higher ($P < 0.05$) systolic BP than Wistar rats, heavy proteinuria ($P < 0.05$, MWF *versus* Wistar), and impaired renal function. Representative images at optical microscopy of histologic cortical renal lesions in these animals, with signs of glomerulosclerosis, are reported in Figure 5B. Using TEM, as shown in Figure 5D, in the preserved areas of the glomerular capillary tuft, the ultrastructure of the glomerular membrane in MWF rats is normal and comparable to that of Wistar rats (Figure 5C).

Morphometric Analysis of Filtration Slit in Proteinuric Rats

In proteinuric animals, we analyzed the structure of filtration slits in preserved areas of capillary loops, which were apparently not affected by podocyte effacement or sclerosis. As shown in Figure 6, the ultrastructure of the filtration slits was very similar to that of Wistar rats.

Morphometric analysis showed that, in MWF rats, slit pore dimensions are similar to that of normal controls. Values of the minor and major radius averaged 10.9 and 14.5 nm, respectively, and mean pore radii were also log-normally distributed (Figure 3B), as in Wistar rats. The mean pore radius of the best fitting log-normal distribution was $u = 11.4$ nm, and the SD of the corresponding normal probability distribution was $s = 1.39$ (Figure 3B). In MWF rats, the majority of pores had an area ranging from 250 to 500 nm^2, as in normal controls, with

a mean pore area of 564 nm^2. Of note, in MWF rats, a small fraction of the pore population was detected to have a large size (>2500 nm^2). The fractional area of these largest pores was 4.7% (Figure 4B).

To further confirm whether the slit pore ultrastructure we observed is also present in other proteinuric conditions, we studied kidney samples from Zucker diabetic fatty (ZDF) rats, a proteinuric model of type 2 diabetes. Three ZDF animals at 8 months of age with proteinuria levels comparable to those of MWF rats (503 ± 80 mg/day) were studied. As shown in Figure 6, we observed the same heteroporous structure of the podocytes slits in these proteinuric animals, confirming that this ultrastructural organization is consistent in the preserved area of the glomerular capillary membrane in different rat strains, both in normal and proteinuric conditions.

DISCUSSION

Conventional SEM could not show the fine details of the ultrastructure of slit openings because secondary electrons can barely escape from the slit that has a deep "u" shape in transversal section, even using high-voltage beam energy. Here, we took advantage of a highly sensitive in-lens detector to capture the electrons emitted from the deepest region of the filtration slits. The electric field of the column, used to decelerate primary electrons near the sample surface, is used by the in-lens detector to accelerate secondary electrons scattered by the surface, thus amplifying the signal produced by emitted electrons with low energy and improving signal-to-noise ratio. Of note, our images were taken using acceleration voltage <0.8 kV, which are values much lower than those used by conventional SEM examination of this type of samples. Finally, the position of the in-lens detector, very close to the primary electron beam and close to the sample, provided better resolution compared with conventional detector that is laterally positioned and more distant from the scanned surface. This highly sensitive technology allowed us to obtain new documentation of the ultrastructure of the outer layer of the glomerular filtration slits. In detail, at variance with previous representations of a regularly spaced ladder such as a structure derived from TEM, we observed a structure characterized by ellipsoidal openings with varying sizes. Of note, when the slit diaphragm is imaged by conventionally TEM, a view perpendicular to the slit major axis is obtained.

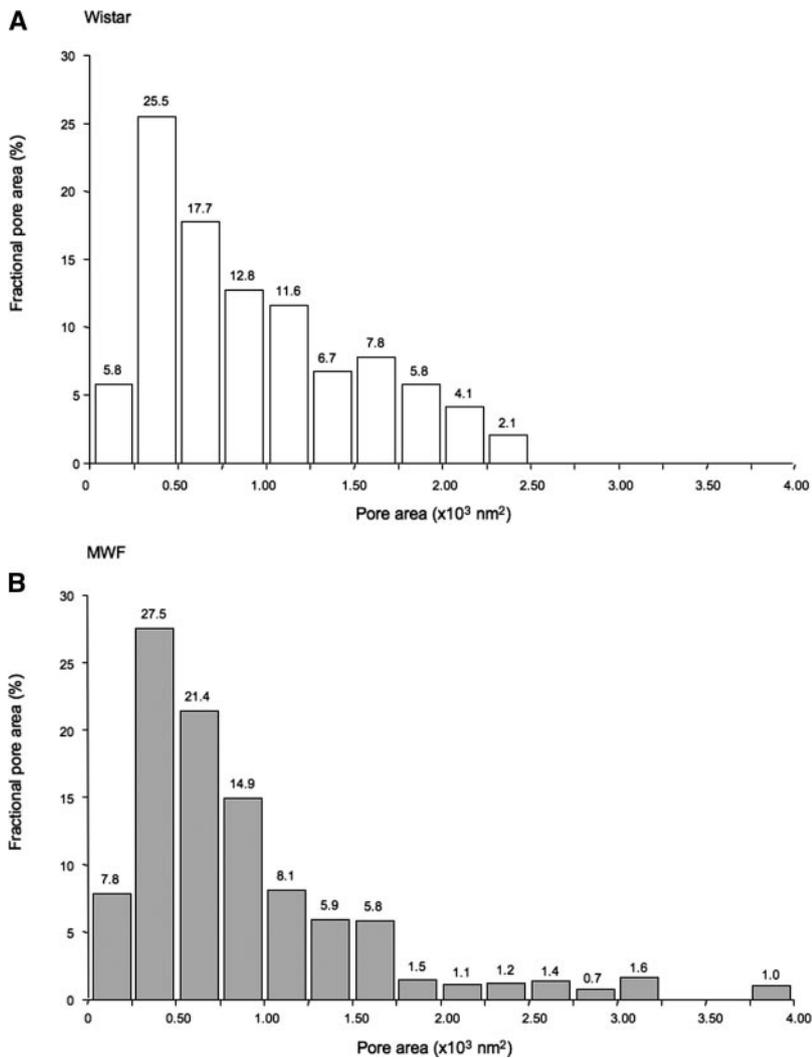Very infrequent observations on the face of the slit have been provided such as those of Rodewald and Karnovsky.[11]

Figure 4. Proteinuric rats contain larger pores. Distribution of fractional pore area (the fraction of total pore area for given pore area interval) calculated for slit pores of Wistar (A) and MWF (B) rats.

The observation plane is parallel to the slit axis in images taken with SEM, in contrast with conventional images taken with TEM. Thus, the different pore structure we observed could depend on the different observation plane of the two techniques, and our present data are not in conflict with the regularity of the slit dimension seen using conventional TEM.

Our direct observation of the organization of the glomerular filtration slit represents an important step toward more deep investigation of the glomerular barrier ultrastructure and

Table 1. Systemic parameters measured in Wistar and MWF rats

Groups	Systolic BP (mmHg)	Urinary Protein Excretion (mg/day)	Serum Creatinine (mg/dl)
Wistar	126 ± 5	17 ± 5	0.56 ± 0.11
MWF	162 ± 3[a]	608 ± 82[a]	0.91 ± 0.25

Values are expressed as mean ± SD. BP, blood pressure.
[a]$P < 0.05$ vs Wistar rats.

function. Our results show that this cell junction is characterized by pores, variable in size and shape, mainly located in the central region of the slit, and not regularly spaced. We verified that this heteroporous structure is not an artifact resulting from technical processing, such as dehydration. Despite the fact that this structure is different from that proposed by Rodewald and Karnovsky,[11] it is compatible with the three-dimensional structure of the protein strands forming irregular elongated pores on both sides of a central denser region proposed by Wartiovaara et al. by microtomography.[15] Both Rodewald and Karnovsky and Wartiovaara et al.[11,15] documented the presence of a central, discontinuous filament in the space between two adjacent podocytes, a structure that we did not observe. It is possible, however, that the pores we visualized by SEM are located inside the discontinuous and irregular strands described by Wartiovaara et al.[15]

On the basis of our morphometric analysis, the slit pore size distribution is remarkably in line with the prediction of hypothetical membrane pore sizes derived from experimental measures of glomerular sieving coefficients of neutral test macromolecules of graded sizes and theoretical analysis.[25,26] Of interest, these studies indicated that the most accurate simulation of experimental and clinical data are obtained assuming membrane pores radii to be lognormally distributed.[5,27] The quantitative analysis performed here on the mean radius of the ellipsoidal openings of the filtration slit indicates a log-normal probability distribution in normal and proteinuric conditions.

However, although the probability distribution of the pores we imaged in the filtration slit is identical to that of hypothetical membrane pores, their dimension is not. Thus, mean pore radius of slit pores we derived in Wistar rats was 12.20 nm, whereas membrane pores derived from sieving coefficients of neutral test macromolecules ranged from 3.5 to 10 nm in different studies.[25,28] One reason for this discrepancy can be that macromolecule passage across the capillary membrane is restricted not only by epithelial layer but also endothelial and glomerular basement membrane layers. Glomerular endothelial cells are fenestrated, and the mean radius of the fenestrae is about 30 nm,[29,30] and is thus not expected to exert significant resistance to macromolecule passage. However, glycoproteins that cover the endothelial fenestrae may exert steric hindrance to the macromolecules pas-
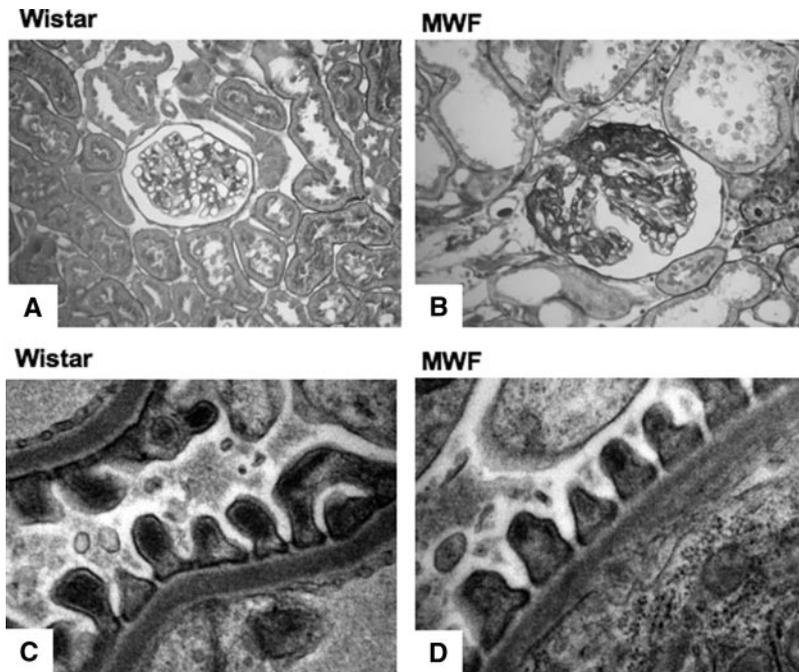
Figure 5. The ultrastructure of the preserved area of glomerular capillary tuft is similar in normal and proteinuric rats. Representative glomerular sections stained by periodic-acid Schiff and transmission electron micrographs of the capillary wall in Wistar (A and C) and MWF (B and D) rats. Original magnifications: 400× (A and B) and 36,000× (C and D).

sage. More importantly, the openings of the glomerular basement membrane protein mesh seem to have variable dimension (from 10 to 20 nm in radius),[31,32] and this structure is expected to contribute, at least in part, to the sieving properties of the capillary membrane, even if experimental evidence suggests that the contribution of the glomerular basement membrane alone on glomerular membrane permeability to macromolecules is less than that of the cellular components (both endothelial and epithelial layer).[33] Thus, the overall sieving coefficient of the glomerular membrane is expected to result from the contribution of these three layers in series, as described in details by Deen and Lazzara.[17] The presence of these hindrance factors before the slit diaphragm reasonably explains the difference in estimated hypothetical membrane pore dimensions and the larger pore dimensions we quantified in the slit diaphragm.

In this study, we also investigated whether the pore ultrastructure in the filtration slit is affected by proteinuric conditions. The heteroporous structure of the podocytes slit was very similar in two different proteinuric conditions (the MWF and ZDF rat) to that of normal rats. Morphometric analysis showed that, in proteinuric MWF rats, slit pore morphology was comparable to that observed in controls, and the ellipsoidal pores have a lognormal distribution of mean pore radii. However, in MWF rats, large pores were observed, larger than those found in the normal condition. It is tempting to speculate that these large openings in the most restrictive layer of the membrane could justify the excessive escape of proteins throughout the glomerular barrier.

We previously also showed[13,20] that some foot process ef-

facement is present in this model of glomerular injury, whereas the remaining portion of the capillary tuft appears normal. We hypothesize that the plasma protein cannot cross the capillary membrane in areas covered by a compact epithelial layer (*i.e.,* process effacement), but they must traverse the membrane through filtration slits.

Using theoretical analysis of neutral dextran fractional clearance data, we previously documented[25] in these animals that restrictive membrane pores (log-normally distributed) are comparable in size to that of normal animals, whereas the importance of the shunt pathway is significantly increased in MWF rats. This pathway is assumed to be a nonselective pore population: large in size but few in number. According to these calculations,[28] the fraction of filtrate passing through the shunt pathway is as low as 0.04%. Previous theoretical models indicated that the presence of a quantitative small shunt pathway explains the appearance of plasma proteins, such as albumin, in the urine.[17] Actually, our present data, for the first time, indicate a potential nature of this shunt pathway that has not been previously identified. The existence of a few large pores in the filtration slits of the MWF rats we documented, which were much larger that albumin and other circulating proteins, might represent the morphologic basis of the shunt pathway. The slit pores of the MWF rats with mean radius >30 nm can easily accommodate the fraction of filtrate that was estimated for the shunt pathways in proteinuric conditions, as membrane hydraulic resistance depends on the pore radius to the third power.

In conclusion, we reported a detailed porous ultrastructure organization of glomerular filtration slits, characterized by ellipsoidal openings with variable dimensions. This new filtration slit imaging indicates that the previously used functional models of porous glomerular membranes have an effective ultrastructural component in the epithelial cell junction. Changes in the ultrastructural organization of the filtration slit may be strictly related to increased ultrafiltration of plasma proteins in glomerular diseases.

CONCISE METHODS

Animals and Experimental Design
This study was performed on kidney samples from three male MWF rats from our colony[34] and three male Wistar rats (Charles River S.p.A., Calco, Italy), healthy and nonproteinuric, used as normal controls. All animals were study at 40 weeks of age. Systolic BP, urinary protein excretion, and serum creatinine were measured by conven-
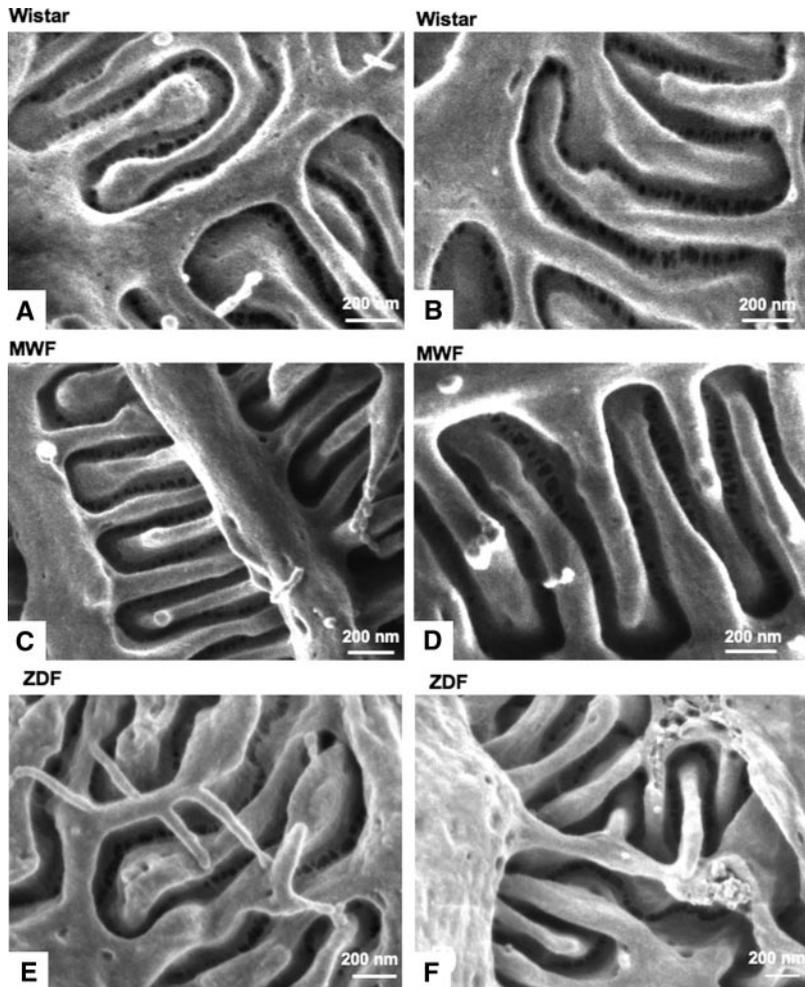
Figure 6. The ultrastructure of the filtration slits is similar in different rat strains, both in normal and proteinuric conditions. Representative scanning electron photomicrographs of filtration slit ultrastructure between neighboring podocytes in Wistar (A and B), MWF (C and D), and ZDF (E and F) rats, taken with an in-lens detector. Original magnifications: A and C, 120,000×; B, 85,000×; D, 150,000×; E, 100,000×; F, 140,000×.

tional methods.[20,24] An additional group of three ZDF rats (Gmi-fa/fa), a model of type 2 diabetes, based on impaired glucose tolerance that leads to insulin resistance, was included in the study. ZDF rats were studied at 8 months, at which time they develop focal segmental glomerulosclerosis, proteinuria, and severe renal failure.[35] All animals were maintained in a temperature-controlled room regulated with a 12-hour light/dark cycle, and they had free access to water and food. Animal care and treatment were conducted in accordance with the institutional guidelines that are in compliance with national (D.L. n.116, G.U. suppl 40, 18-2-1992, Circ n.8, G.U. 14-7-1994) and international laws and policies (EEC Council Dir. 86/609, OJL 358-1, 1987; *Guide for the Care and Use of Laboratory Animals,* U.S. N.R.C., 1996).

At death, kidneys were obtained and processed for morphologic evaluation by perfusion fixation. Briefly, rats were anesthetized and opened through a midline incision. The abdominal aorta was cannulated below the renal arteries with a catheter connected to a pressure transducer (Battaglia Rangoni, Bologna, Italy). Both kidneys were perfused with PBS at the measured arterial pressure for 3 to 5 minutes. Kidneys were perfused with 1.25% glutaraldehyde in 0.1 M cacodylate buffer at the same pressure for 5 minutes and removed. For histologic evaluations, midcoronal sections were postfixed overnight in Dubosq-Brazil, dehydrated in alcohol, and embedded in paraffin. Kidney samples were sectioned at 3-μm intervals with a Leica RM 2255 microtome (Leica Microsystems, Milan, Italy) and stained with periodic-acid Schiff reagent.

TEM

For TEM analysis, kidney tissue was removed and cut in small pieces (1 mm^3), which were immersed in 2.5% glutaraldehyde in 0.1 M cacodylate buffer (pH 7.4), for 4 hours at room temperature, washed in cacodylate buffer, and postfixed with 1% OsO$_4$ for an additional hour. Fixed specimens were dehydrated through ascending grades of alcohol and embedded in Epon resin. Ultrathin sections (100 nm) were cut on an ultramicrotome (LKB Instruments, Bromma, Sweden), collected on copper grids, and stained with uranyl acetate and lead citrate. Ultrastructural evaluations were performed by a transmission Morgagni 268D electron microscopy (FEI Company, Eindhoven, The Netherlands).

SEM

For SEM analysis, midcoronal sections of the kidneys were postfixed overnight in 2.5% glutaraldehyde (buffered with 0.1 M sodium cacodylate buffer, pH 7.4). Sections were repeatedly washed in cacodylate buffer and postfixed in 1% osmium tetroxide for 1 hour. Fixed specimens were dehydrated with increasing concentrations of alcohol. Immediately after dehydration, samples were rinsed with liquid CO$_2$ with a Bal-Tec 030 critical point dryer (BAL-TEC AG, Balzers, Liechtenstein) or dehydrated in pure HMDS (Polyscience) (twice for 0.5 hours), which permitted reaching the critical point of dehydration in a less aggressive way.[22,23] Samples were mounted on stubs and coated with gold in a sputter coater (Agar Scientific, Stansted, UK). In parallel, some kidney samples were used for SEM without gold coating, for comparison. Acceleration voltage was set to 0.4 to 0.8 kV and enlargement up to 350 kx.

Ultrastructure Morphometric Analysis

Three glomeruli per animals were analyzed. Imaging fields, from the well-preserved areas of glomerular capillary tuft, were randomly taken, and all measurements were provided in pores, independently of their localization along the foot process. The estimation of the size of slit pores was performed on digitized images using NIH Image J

software and a Mac OS PC (Apple Computer, Cupertino, CA). For each digital image (1024 × 768 pixel) obtained with SEM, a surface plot area (RGB) of selected region of interest was performed, as representatively shown in Figure 2. The surface plot displays a three-dimensional graph of the intensities of pixels in a pseudocolor image. The use of different colors facilitated identification of the pores edges and thus their size quantification. For each pore, the diameters (major and minor) were manually outlined on the surface plot, along the *x* and *y* axis (Figure 2), using a line and automatically measured in screen pixel. This value was converted in nanometers using exact enlargement on each photomicrograph. The quantification of pore sizes was performed on 596 pores imaged from samples of Wistar rats and on 735 pores of sample from MWF rats.

Statistical Analysis
Systemic parameters, expressed as mean ± SD, were analyzed using the nonparametric Kruskal-Wallis test. The statistical significance level was defined as $P < 0.05$.

ACKNOWLEDGMENTS

DISCLOSURES

None.

REFERENCES

1. Deen WM, Lazzara MJ, Myers BD: Structural determinants of glomerular permeability. *Am J Physiol Renal Physiol* 281: F579–F596, 2001
2. Edwards A, Daniels BS, Deen WM: Ultrastructural model for size selectivity in glomerular filtration. *Am J Physiol* 276: F892–F902, 1999
3. Abbate M, Zoja C, Remuzzi G: How does proteinuria cause progressive renal damage? *J Am Soc Nephrol* 17: 2974–2984, 2006
4. Sorensson J, Ohlson M, Haraldsson B: A quantitative analysis of the glomerular charge barrier in the rat. *Am J Physiol Renal Physiol* 280: F646–F656, 2001
5. Remuzzi A, Battaglia C, Rossi L, Zoja C, Remuzzi G: Glomerular size selectivity in nephrotic rats exposed to diets with different protein content. *Am J Physiol* 253: F318–F327, 1987
6. Jeansson M, Haraldsson B: Glomerular size and charge selectivity in the mouse after exposure to glucosaminoglycan-degrading enzymes. *J Am Soc Nephrol* 14: 1756–1765, 2003
7. Tojo A, Endou H: Intrarenal handling of proteins in rats using fractional micropuncture technique. *Am J Physiol* 263: F601–F606, 1992
8. Tanner GA: Glomerular sieving coefficient of serum albumin in the rat: A two-photon microscopy study. *Am J Physiol Renal Physiol* 296: F1258–F1265, 2009
9. Remuzzi A, Sangalli F, Fassi A, Remuzzi G: Albumin concentration in the Bowman's capsule: Multiphoton microscopy vs micropuncture technique. *Kidney Int* 72: 1410–1411, 2007
10. Peti-Peterdi J: Independent two-photon measurements of albumin GSC give low values. *Am J Physiol Renal Physiol* 296: F1255–F1257, 2009
11. Rodewald R, Karnovsky MJ: Porous substructure of the glomerular slit diaphragm in the rat and mouse. *J Cell Biol* 60: 423–433, 1974
12. Remuzzi A, Monaci N, Bonassi ME, Corna D, Zoja C, Mohammed EI, Remuzzi G: Angiotensin-converting enzyme inhibition prevents loss of glomerular hydraulic permeability in passive heymann nephritis. *Lab Invest* 79: 1501–1510, 1999
13. Iordache BE, Imberti O, Foglieni C, Remuzzi G, Bertani T, Remuzzi A: Effects of angiotensin-converting enzyme inhibition on glomerular capillary wall ultrastructure in MWF/Ztm rats. *J Am Soc Nephrol* 5: 1378–1384, 1994
14. Benigni A, Gagliardini E, Tomasoni S, Abbate M, Ruggenenti P, Kalluri R, Remuzzi G: Selective impairment of gene expression and assembly of nephrin in human diabetic nephropathy. *Kidney Int* 65: 2193–2200, 2004
15. Wartiovaara J, Ofverstedt LG, Khoshnoodi J, Zhang J, Makela E, Sandin S, Ruotsalainen V, Cheng RH, Jalanko H, Skoglund U, Tryggvason K: Nephrin strands contribute to a porous slit diaphragm scaffold as revealed by electron tomography. *J Clin Invest* 114: 1475–1483, 2004
16. Sugio S, Kashima A, Mochizuki S, Noda M, Kobayashi K: Crystal structure of human serum albumin at 2.5 A resolution. *Protein Eng* 12: 439–446, 1999
17. Deen WM, Lazzara MJ: Glomerular filtration of albumin: how small is the sieving coefficient? *Kidney Int Suppl*: S63–S64, 2004
18. Lazzara MJ, Deen WM: Model of albumin reabsorption in the proximal tubule. *Am J Physiol Renal Physiol* 292: F430–F439, 2007
19. Hora K, Ohno S, Oguchi H, Furukawa T, Furuta S: Three-dimensional study of glomerular slit diaphragm by the quick-freezing and deep-etching replica method. *Eur J Cell Biol* 53: 402–406, 1990
20. Macconi D, Bonomelli M, Benigni A, Plati T, Sangalli F, Longaretti L, Conti S, Kawachi H, Hill P, Remuzzi G, Remuzzi A: Pathophysiologic implications of reduced podocyte number in a rat model of progressive glomerular injury. *Am J Pathol* 168: 42–54, 2006
21. Cazaux J: About the role of the various types of secondary electrons (SE; SE; SE) on the performance of LVSEM. *J Microsc* 214: 341–347, 2004
22. Brown B: A further chemical alternative to critical-point-drying for preparing small (or large) flies. *Fly Times* 11: 10, 1993
23. Bray DF, Bagu J, Koegler P: Comparison of hexamethyldisilazane (HMDS), Peldri II, and critical-point drying methods for scanning electron microscopy of biological specimens. *Microsc Res Tech* 26: 489–495, 1993
24. Macconi D, Sangalli F, Bonomelli M, Conti S, Condorelli L, Gagliardini E, Remuzzi G, Remuzzi A: Podocyte repopulation contributes to regression of glomerular injury induced by ACE inhibition. *Am J Pathol* 174: 797–807, 2009
25. Remuzzi A, Puntorieri S, Battaglia C, Bertani T, Remuzzi G: Angiotensin converting enzyme inhibition ameliorates glomerular filtration of macromolecules and water and lessens glomerular injury in the rat. *J Clin Invest* 85: 541–549, 1990
26. Deen WM, Bridges CR, Brenner BM, Myers BD: Heteroporous model of glomerular size selectivity: Application to normal and nephrotic humans. *Am J Physiol* 249: F374–F389, 1985
27. Ruggenenti P, Mosconi L, Sangalli F, Casiraghi F, Gambara V, Remuzzi G, Remuzzi A: Glomerular size-selective dysfunction in NIDDM is not ameliorated by ACE inhibition or by calcium channel blockade. *Kidney Int* 55: 984–994, 1999
28. Haraldsson B, Nystrom J, Deen WM: Properties of the glomerular barrier and mechanisms of proteinuria. *Physiol Rev* 88: 451–487, 2008
29. Drumond MC, Deen WM: Structural determinants of glomerular hydraulic permeability. *Am J Physiol* 266: F1–F12, 1994
30. Lea PJ, Silverman M, Hegele R, Hollenberg MJ: Tridimensional ultrastructure of glomerular capillary endothelium revealed by high-reso-

lution scanning electron microscopy. *Microvasc Res* 38: 296–308, 1989

31. Hironaka K, Makino H, Yamasaki Y, Ota Z: Pores in the glomerular basement membrane revealed by ultrahigh-resolution scanning electron microscopy. *Nephron* 64: 647–649, 1993

32. Palassini M, Remuzzi A: Numerical analysis of viscous flow through fibrous media: A model for glomerular basement membrane permeability. *Am J Physiol* 274: F223–F231, 1998

33. Edwards A, Deen WM, Daniels BS: Hindered transport of macromolecules in isolated glomeruli. I. Diffusion across intact and cell-free capillaries. *Biophys J* 72: 204–213, 1997

34. Remuzzi A, Puntorieri S, Alfano M, Macconi D, Abbate M, Bertani T, Remuzzi G: Pathophysiologic implications of proteinuria in a rat model of progressive glomerular injury. *Lab Invest* 67: 572–579, 1992

35. Baylis C, Atzpodien EA, Freshour G, Engels K: Peroxisome proliferator-activated receptor [gamma] agonist provides superior renal protection versus angiotensin-converting enzyme inhibition in a rat model of type 2 diabetes with obesity. *J Pharmacol Exp Ther* 307: 854–860, 2003